

# 양단 공진과 듀티 컨트롤을 이용한 1-2cm 공극을 통한 에너지 전달

김 창균<sup>o</sup>, 조 보형  
서울대학교 공과대학 전기공학부

## Transcutaneous Energy Transmission with Double Tuned Duty Cycle Control

Chang-Gyun Kim<sup>o</sup>, Bo-Hyung Cho  
School of Electrical Engineering, Seoul National University

### 1. ABSTRACT

A dc-dc converter which transfers 12-48W of power (regulated output voltage 24V) across a large, variable air gap (1-2cm) has been designed. This converter employs double resonance to compensate the large leakage inductance of the primary and secondary of the transcutaneous transformer. To maximize the effect of resonance, a constant frequency, duty cycle control method is used. The duty cycle control presents advantages over a frequency control in terms of increase in dc voltage gain and reduction of the primary current. The analysis and design procedure for the proposed scheme is presented and the performance result is simulated and verified experimentally.

### 2. INTRODUCTION

There has been a great deal of researches on transferring electric energy from outside the human body to an internal motor driven artificial heart.[1-4] It would be desirable to transfer a required electrical power for the circulatory device inside of the patient's body using electromagnetic coupling without breaking the skin. This method of energy transfer is called transcutaneous energy transmission.

The gap between the primary and secondary windings of a transcutaneous transformer depends on the thickness of the patient's skin, which normally varies between one and two centimeters[1].

This large gap results in a very low coupling coefficient of the transformer and the magnetizing inductance of the transformer is usually much lower than the leakage inductance. In fact, the leakage inductance is 2-5 times larger than the magnetizing inductance for the given air gap specification. This means that the transference of energy through this transcutaneous transformer is not efficient for two main reasons: low transfer gain of voltage, and large circulating current through the transformer and the primary circuit. The low voltage gain causes a higher battery voltage and the large circulating current causes low efficiency.

In this paper, a constant frequency duty cycle controlled double tuned circuit is proposed to maximize the voltage gain and the efficiency of the system.

### 3. ANALYSIS OF THE PROPOSED SCHEME

#### 3.1 Double Tuned Circuit

Fig.1 shows the proposed scheme. To transfer energy effectively, a high voltage gain and small circulating current are essential. To obtain a high voltage gain and small circulating current, two capacitors, C1 and C2, are added in series with the primary and secondary leakage inductances, L1 and L2. Each capacitor resonates with the primary and secondary leakage inductances, respectively, and compensates the impedance of the large leakage inductance by setting the operating frequency near the resonant frequencies. This can increase the voltage gain and decrease the primary circulating current.

#### 3.2 Dc Voltage Gain And Primary Current

The dc input voltage is converted to a quasi square wave by full bridge switches to excite the transformer primary coil as shown in the Fig. 1. The loaded transformer presents a low impedance at the fundamental frequency of the square wave and relatively high impedance at the frequencies of the higher harmonics. Thus, the primary current wave form approximates the fundamental sine wave. Using the simplified

circuit shown in Fig. 2, the voltage gain is derived from the fact that the quasi square wave is expanded by sine waves, where the rectifier diodes, output filter capacitor, and the load resistor are modeled by a simple equivalent resistor  $R_e$ [5].

$$\frac{V_2}{V_1} = N \left[ \left( 1 + \frac{1-k}{k} \left( 1 - \frac{1}{\omega_1^2} \right) \right)^2 + \frac{\omega_1^2}{\omega_2^2} Q^2 \left[ \left( 2 - \frac{1}{\omega_1^2} - \frac{1}{\omega_2^2} \right) + \frac{1-k}{k} \left( 1 - \frac{1}{\omega_1^2} \right) \left( 1 - \frac{1}{\omega_2^2} \right) \right] \right]^{-\frac{1}{2}} \quad (1)$$

where,

$$\omega_1 = \frac{\omega_0}{Q}, \quad \omega_2 = \frac{\omega_0}{Q}, \quad \omega_0 = 2\pi f_0$$

$$\omega_1 = \frac{1}{\sqrt{L_1 C_1}}, \quad \omega_2 = \frac{1}{\sqrt{L_2 C_2}}, \quad Q = \frac{\omega_0 L_2}{R_e}, \quad R_e = \frac{R_L}{k^2}$$

$$k = \frac{L_m}{\sqrt{(L_1 + L_m)(L_2 + L_m)}} \quad N = N_2 / N_1$$

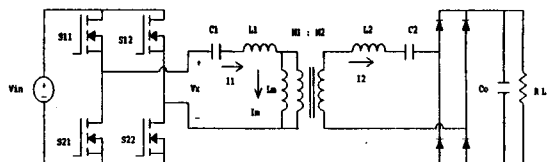


FIG. 1 THE POWER STAGE CIRCUIT

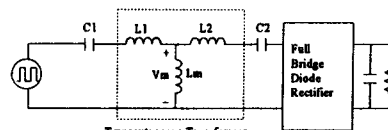


FIG. 2 SIMPLIFIED CIRCUIT

The primary current,  $I_1$  which passes through the switches, is the vector sum of the magnetizing current and the secondary current. The secondary current is determined by the required load current and magnetizing current is determined by the transformer voltage,  $V_m$  in Fig.2, which depends on the output voltage and the voltage on the L2, C2. Assuming the currents through L1, L2, and  $L_m$  are sine wave form, the primary current is derived as Eq (2).

$$I_1 = \left[ \left( \frac{\pi V_m N}{2R} \left( 1 + \frac{1-k}{k} \left( 1 - \frac{1}{\omega_1^2} \right) \right) \right)^2 + \left( \frac{4V_m N}{\pi R_e Q} \left( 1 - \frac{1}{\omega_2^2} \right) \right)^2 \right]^{\frac{1}{2}} \quad (2)$$

From Eq.(1), the voltage gain depends on the normalized primary and secondary resonant frequencies and the Q factor. In general, for a high voltage gain, these resonant frequencies must be placed near unity. As the Q increases, which implies increase in the operating frequency for a fixed  $\omega_1$ , the voltage gain decreases. However, from Eq.(2) increase in the Q results smaller primary current. This is because for a given load current, higher Q results in an increase of impedance of the magnetizing inductance.

The primary current also depends on  $\omega_2$ . The primary current is the vector sum of the magnetizing and load currents. As the operating frequency is above the secondary resonant frequency ( $\omega_2 > 1$ ) the secondary resonant branch has the property of inductance, and the load current and the magnetizing current both lag. This results a large primary current as shown in Fig. 5(a). As the operating frequency decreases ( $\omega_2 < 1$ ), the secondary resonant branch has the property of capacitance and the phase difference between the load and magnetizing current becomes large. This makes the primary current small (Fig. 5(b)). As the normalized secondary resonant frequency continuously decreases beyond a critical frequency, impedance of the secondary resonant branch increases, and thus the primary current increases as shown in Fig. 4. This critical frequency for the minimum primary current can be found by differentiating Eq. (2).

$$\omega_{r2} = \sqrt{1-k} \quad (3)$$

Also, the voltage gain and the primary current depend on the relative position of  $\omega_{r1}$  and  $\omega_{r2}$ . Thus a trade-off between the voltage gain and the primary current with respect to  $\omega_{r1}$ ,  $\omega_{r2}$  and the Q factor must be considered.

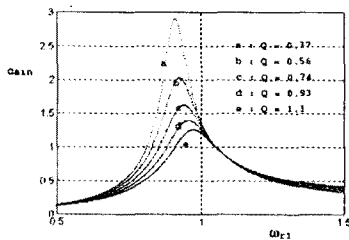


FIG. 3 VOLTAGE GAIN VS  $\omega_{r1}$  ( $\omega_{r2} = 0.96$ )

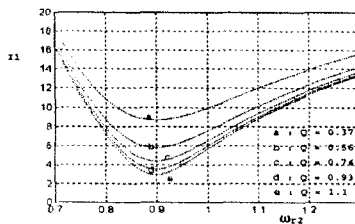


FIG. 4 PRIMARY CURRENT VS  $\omega_{r2}$

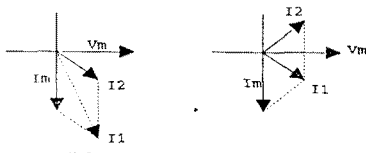


FIG. 5 PHASE DIAGRAM OF THE PRIMARY, SECONDARY, AND MAGNETIZING CURRENT

### 3.3 Output Voltage Control

In order to regulate the output voltage for varying load and air gap, either the frequency control or the duty cycle control method can be used. To use frequency control, the operating frequency must be above the primary and the secondary resonant frequencies and have wide frequency range [1]. Thus it cannot fully utilize the double resonance for a higher voltage gain and a lower circulating current. Also the restriction that the operating frequency must be above the secondary resonant frequency ( $\omega_2 > 1$ ) causes a large primary current as discussed in Sec. 3.2.

To solve these problems, a constant frequency duty cycle control method is proposed. In this method, the ON-time of the switches in the primary bridge is controlled to generate a quasi-square wave as shown in the Fig. 6. For this control method, the operating frequency can be fixed near the resonant frequency in order to maximize the effect of resonance, and the output voltage is controlled by the duty cycle of the primary switches. To minimize the input current the operating frequency should be placed below the secondary resonant frequency.

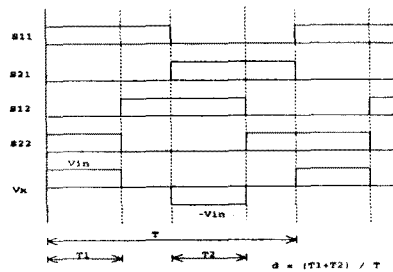


FIG. 6 DUTY CYCLE CONTROL

## 4. DESIGN PROCEDURE

### 4.1 Transcutaneous Transformer

Transcutaneous transformer has an inherent large air gap and this causes a large leakage flux. In order to reduce the leakage flux and increase the coupling coefficient, it is necessary to use a large size magnetic core. A transformer with a particular geometry was designed to maximize the coupling. The transformer has a large cross sectional area which contacts with the air gap and small cross sectional area otherwise as shown in Fig. 7. This geometry results in less dependency on varying air gap and a smaller transformer size and weight than the one used in [1]. The transformer design results are in Table 1.

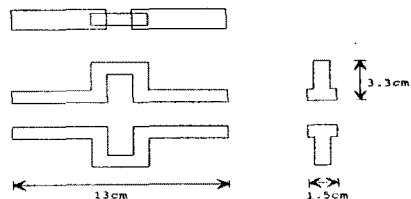


FIG. 7 THE TRANSCUTANEOUS TRANSFORMER

TABLE 1. TRANSFORMER DESIGN RESULTS

air gap	k	L1	L2	Lm
1cm	0.32	29.6uH	67.9uH	13.7uH
2cm	0.19	32.7uH	72.1uH	7.67uH

### 4.2 The Primary Side Resonant Frequency, Secondary Side Resonant Frequency And Operating Frequency

The design procedure is as follows: First, from Fig. 4,  $\omega_{r2}$  and Q (operating frequency) can be selected for a proper primary current level by considering the primary switch's current capacity and its switching speed. As discussed in Sec. 3.1, a trade-off between the voltage gain which affects the battery voltage, and the primary current level for an efficiency requirement must be considered. This can be done through several iteration process to find a desired selection. The switching frequency,  $f_s$  of 100kHz ( $Q=0.74$ ) is selected, above which the primary current level does not decrease much. Once  $f_s$  is selected, the primary current as a function of  $\omega_{r2}$  is plotted in Fig. 8 for the extreme values of k and R. For the voltage gain, for every  $\omega_{r2}$ , the maximum voltage gain of the smallest gain among the four extreme conditions (k and R) can be found by sweeping  $\omega_{r1}$ . The results are shown in Fig. 9. By comparing Fig. 8 and Fig. 9  $\omega_{r2}$  can be selected to satisfy both the voltage gain and the current requirements. In this design,  $\omega_{r2}$  of 0.96 is selected.

Fig. 10 shows the voltage gain as a function of  $\omega_{r1}$  for a selected  $\omega_{r2} = 0.96$ . As explained above, the maximum of the smallest gain among the four cases is at  $\omega_{r1} = 1.02$ .

The designed value of  $f_s$ ,  $f_{r1}$ ,  $f_{r2}$  and C1, C2 are in Table 2

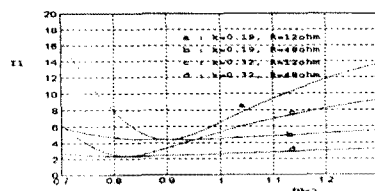


FIG. 8 THE PRIMARY CURRENT VS  $\omega_{r2}$  ( $F_s=100KHZ$ )

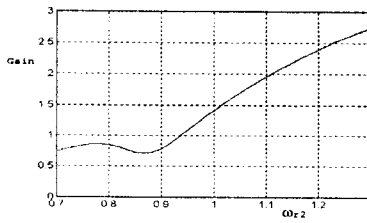


FIG. 9 THE MAXIMUM VOLTAGE GAIN OF THE SMALLEST GAIN AMONG THE FOUR EXTREME CONDITIONS (K AND R)

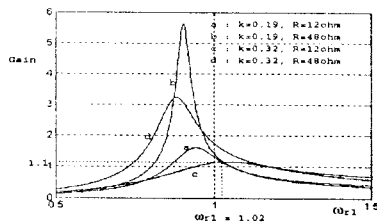


FIG. 10 THE VOLTAGE GAIN VS  $\omega r_1$  ( $\omega r_2 = 0.96$ ,  $F_s = 100\text{KHZ}$ )

TABLE 2. DESIGNED VALUE OF  $F_s$ ,  $F_{r1}$ ,  $F_{r2}$ ,  $C_1$ , AND  $C_2$

$F_s$	$F_{r1}$	$F_{r2}$	$C_1$	$C_2$
100kHz	1.02	0.96	82nF	32nF

## 5. PERFORMANCE RESULTS

For the designed value, the voltage gain curve vs. duty ratio is in Fig. 11. The maximum duty ratio is set at  $D_{max}=0.8$  and Fig. 11 shows that the minimum gain among the four cases is 1.1. Thus the minimum battery voltage  $V_{batmin}$  can be designed as 22V. Since this analysis does not include losses in the power circuit, the actual  $V_{batmin}$  should be higher than 22V, taking into consideration of the efficiency. Theoretical prediction of the worst case peak switch current is 5.5A and Fig. 14 shows the oscillogram under the worst case condition, which shows the peak switch current of 5A. The previous work[1] which uses the single resonant, frequency control shows that the voltage gain is 0.17 and the peak input current is 8A with  $V_{bat}$  of 145V.

For the control loop design, the empirical small-signal modeling technique[6] was employed to get the control to output transfer function. The simulated and experimental results are in Fig. 12. Based on the transfer function characteristic a compensation circuit is designed to ensure the closed loop stability and optimum dynamic performance. The closed loop transfer function is in Fig. 13. Fig. 14 shows the experimental results of the input voltage of the resonant branch ( $V_x$  in Fig. 1) and the primary current ( $I_1$  in Fig. 1). The dynamic response of the output voltage for the step load is shown in Fig. 15.

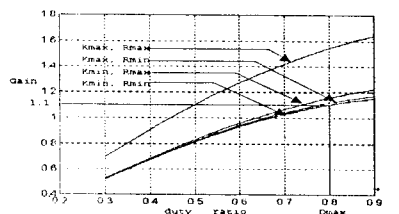


FIG. 11 VOLTAGE GAIN VS DUTY RATIO

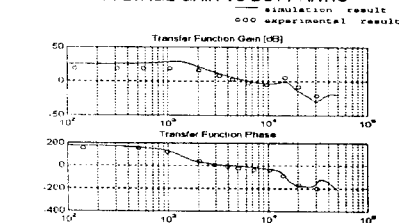


FIG. 12 CONTROL TO OUTPUT TRANSFER FUNCTION

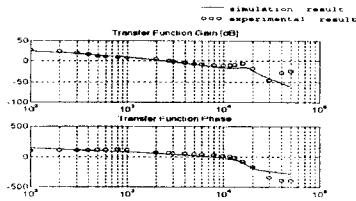


FIG. 13 CLOSED LOOP TRANSFER FUNCTION

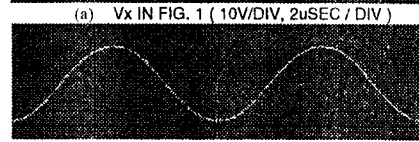
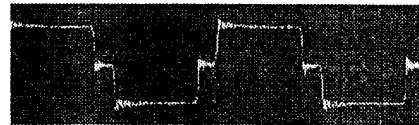


FIG. 14 EXPERIMENTAL VOLTAGE AND CURRENT WAVE FORM ( $V_{out} = 24\text{V}$ ,  $R = 12\text{ohm}$ , AIR GAP = 2cm)

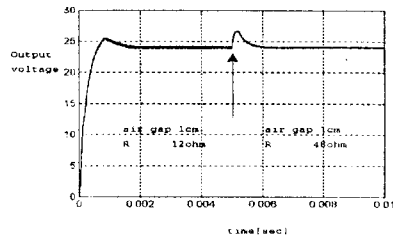


FIG. 15 DYNAMIC RESPONSE FOR STEP LOAD

## 6. CONCLUSION

Compensation of the large leakage inductance due to large air gap employing the double resonance improves the voltage gain and efficiency. The duty cycle control not only maximize the effect of the resonance but also decreases the primary current by properly placing the operating frequency, with respect to the secondary resonant frequency.

## REFERENCES

- [1] A. Ghahary, and B. H. Cho, "Design of a Transcutaneous Energy Transmission System Using a Series Resonant Converter," *IEEE Transactions on Power Electronics*, Vol. 7, No. 2, April, 1992.
- [2] Y. Mitamura, E. Okamoto, A. Hirano, and T. Mikami, "Development of an Implantable Motor-Driven Assist Pump System," *IEEE Transactions on Biomedical Engineering*, Vol. 37, No. 2, Feb. 1990.
- [3] J.C. Schuder, and H.E. Stephenson, "Energy transport to a coil which circumscribes a ferrite core and is implanted within the body," *IEEE Trans. Bio-Med. Eng.*, Vol. BME-12, Nos3 and 4, pp. 154-163, 1965.
- [4] A. Thumin, G. Reed, F. Lupo, G. Myers, and L. Cortes, "A power transformer for mechanical heart," *Artificial Heart Program Conf. Proceedings*, US Government Printing Office, Chap. 77, 1966.
- [5] I. J. Pitel, "Phase-modulated resonant power conversion techniques for high frequency link inverters," *IEEE Trans. Industry Applications*, Vol. IA-22, No. 6, pp. 1044-1051, 1986.
- [6] P. Huynh, and B. H. Cho, "Empirical Small-Signal Modeling of Switching Converters Using Pspice," *IEEE PESC*, June, 1995.